

Corrosion Resistance of NdDyFeB Basic Alloys

Korozijska obstojnost osnovnih zlitin NdDyFeB

S. Kobe Beseničar¹, IJS Ljubljana, Slovenija

L. Vehovar, IMT Ljubljana, Slovenija

B. Saje, Magneti d.d. Ljubljana, Slovenija

Prejem rokopisa - received: 1996-10-01; sprejem za objavo - accepted for publication: 1996-11-04

Nd-Dy-Fe-B-X (X = Zr, Hf) alloys were exposed to severe corrosion conditions and the corrosion rates were followed by various techniques (electrochemistry, Tafel extrapolation method). The weight loss was measured over a period of 10 weeks in a wet corrosion chamber. Corrosion products were analysed using X-ray diffraction and the microstructures were investigated by optical microscopy and on SEM - EDS. In aggressive media, such as diluted NaCl or H₂SO₄, the differences between the corrosion rates were small. The lowest potential difference between the anodic phase (corrosion products) and the matrix, acting as cathode, was observed in Nd-Dy-Fe-B-Zr alloys. Corrosion rates in fresh water were 0,30 mm/year for Nd-Dy-Fe-B alloy and 0,02 mm/year for Nd-Dy-Fe-B-Zr alloy. The same trend was shown on samples exposed to conditions of simulated condensed atmospheric humidity. The highest cumulative weight loss occurred with pure Nd-Dy-Fe-B alloys and the lowest with the alloy improved by ZrO₂ addition. The corrosion rates for three different alloys were 0,089 mm/year for Nd-Dy-Fe-B alloy, 0,072 mm/year for Nd-Dy-Fe-B-Hf alloy and 0,063 mm/year for Nd-Dy-Fe-B-Zr alloy.

Key words: corrosion, Nd-Fe-B alloys, permanent magnets

Osnovne zlitine Nd-Dy-Fe-B-X (X = Zr, Hf) smo izpostavili agresivnim korozijskim pogojem in zasledovali korozijski proces z različnimi metodami (elektrokemija, Taflova ekstrapolacijska metoda). V vlažni komori smo merili izgubo teže v obdobju desetih tednov. Korozijske produkte smo analizirali z uporabo X-žarkovne difrakcije ter opazovanjem mikrostrukture z optično mikroskopijo in elektronskim mikroskopom opremljenim z EDS. V agresivnih medijih kot sta NaCl in H₂SO₄ so bile razlike v korozijski hitrosti med različnimi zlitinami majhne. Najmanjšo razliko potenciala med anodno fazo (korozijski produkt) in matrico, ki deluje kot katoda, smo opazili pri zlitini Nd-Dy-Fe-B-Zr. Korozijska hitrost v vodi je bila 0,30 mm/leto pri zlitinah Nd-Dy-Fe-B in 0,02 mm/leto pri zlitinah Nd-Dy-Fe-B-Zr. Enako tendenco smo opazili pri eksperimentih, pri katerih so bile zlitine izpostavljene pogojem, ki so simulirali nasičeno zračno vlago. Najvišja kumulativna izguba teže je bila dosežena s čistimi Nd-Dy-Fe-B zlitinami in najnižja z Nd-Dy-Fe-B-Zr zlitinami. Korozijske hitrosti za različne zlitine so bile 0,089 mm/leto za zlitino brez dodatkov, 0,072 mm/leto za zlitino z dodatkom HfO₂ in 0,063 mm/leto za zlitino z dodatkom cirkon oksida.

Ključne besede: korozija, Nd-Fe-B zlitine, trajni magneti

1 Introduction

Among the rare earth based permanent magnets, Nd-Fe-B magnets have assumed an important position due to their outstanding magnetic properties^{1,2} and their use is still on growing in different fields of application³. However, corrosion has been a problem with Nd-Fe-B magnets, because phases rich in rare earth elements are easily oxidised in air, especially in humid air^{4,5}. Since corrosion can deteriorate seriously the magnetic properties and on the other hand, can also be detrimental to magnetic circuits, much effort has been made to improve the corrosion resistance of Nd-Fe-B magnets. Even coating and plating are not the perfect solution to this problem, because they can be imperfect and allow the penetration of reacting species such as moisture to the magnet surface⁶. Searching for a better resistance of the material itself, various referred possibilities have been studied.

Narasimhan et al.⁷ reported that raising the oxygen content to between 0,6 to 3,5% significantly improved the corrosion resistance; Kim and Jacobson reported that the addition of Al, Dy or Dy₂O₃ improved the corrosion resistance in humid air⁴, while Tenaud, Vial, Sagawa⁸ and Hirose et al.⁹ used V and Mo to improve the basic

corrosion resistance of Nd-Fe-B magnets. Kobe et al. reported on the beneficial influence of ZrO₂ addition not only to the increased coercivity, but also to the corrosion resistance of the Nd-Dy-Fe-B magnets¹⁰. Previously Nakamura¹¹ attained better corrosion resistance of the Nd-rich phase by the substitution of Fe with Co and Zr, and Sagawa et al.¹² improved the corrosion resistance by addition of Co and Al. Kim et al.⁶ influenced the corrosion resistance by varying the amount of O, C and N in the basic composition of Nd-Fe-B magnets.

On the basis of the promising results in our previous work¹⁰, we continued our studies on the influence of ZrO₂ and HfO₂ additions on improving the corrosion resistance of the basic Nd-Dy-Fe-B alloy with the composition Nd₁₅Dy₁Fe₇₆B₈. The corrosion resistance was followed over experimental periods during which the samples were exposed to various severe corrosion conditions.

2 Experimental

The basic alloys used for the corrosion experiments were prepared by arc melting the alloys NdFe, DyFe, FeB and Fe powder in a pure Ar atmosphere. In order to prevent the oxidation Ti sponge was used as a getter for oxygen. Three different batches were prepared: **A** - samples without other additives, **B** - 1 wt.% hafnia was

¹ Dr. Spomenka KOBESBENIČAR
Inštitut Jožef Stefan, Jamova 39
1001 Ljubljana, Slovenija

added before arc melting, C - 1 wt.% of zirconia was added prior to arc melting. Samples were remelted three times in order to attain a better homogeneity. Buttons of melted alloys were sliced and polished to discs, dimensionally appropriate for the corrosion tests.

The investigations were focused on general corrosion resistance, based on electrochemical determinations of the possible passivity of electrode surfaces, or active corrosion. Moreover, service conditions were simulated by exposing the test specimens in a wet corrosion facility (DIN 5017), with the aim of establishing the effect of chemical composition and microstructure on the corrosion rate and the form of corrosion.

The potentiodynamic anodic polarisation measurements were performed using an EG and G-PAR potentiostat and "Softcorr 352" software. Experiments were carried out in fresh water and in various aqueous test-solutions containing low concentrations of aggressive ions such as Cl⁻ and SO₄²⁻. Such media could only represent approximative atmospheric conditions in the industrial environment. Electrochemical determination of corrosion rates were performed by the Tafel plot technique.

After exposing the samples to various corrosion conditions they were characterised by optical and electron microscopy (SEM/EPMA JEOL, JXA 840 A). Phases in corrosion products were identified using EDS and WDS analysis facilities and an X-ray diffractometry (Philips 1710).

3 Results and discussion

3.1 Effect of the HfO₂ and ZrO₂ additives on the corrosion rate of Nd-Dy-Fe-B alloys

The example of the anodic polarisations curves presented in **Figure 1** indicates that all of the three materials cannot achieve passivity. The overall shape of the curves indicates that the materials undergo active corrosion. It is evident that the potentiodynamic scans did not reveal any significant feature, such as a passive region where passivation is spontaneous, the pitting potential or the critical anodic current. The conclusion from the anodic po-

tentiodynamic scans of the materials carried out in different solutions was that no significant passivation occurred.

Due to such polarisation behaviour of the materials, corrosion rate measurements were performed by the Tafel plot technique. The corrosion rates of the materials tested when exposed in various media are presented in **Table 1** and graphically in **Figure 2**.

From these results it can be concluded that chloride ions drastically promote corrosion. As their concentration increases, so does the rate of corrosion. The corrosion process is also particularly dramatic in acid solutions containing SO₄²⁻ ions, which represent very aggressive industrial atmosphere. The corrosion rates of all materials in fresh water are relatively favourable. In addition, the results of this investigation showed that a defined trend which favours a NDFB-ZrO₂ material exists (**Figure 3, Table 1**).

The same trend among the materials was observed by exposure in a wet corrosion facility, but a substantial improvement of the corrosion properties by addition of ZrO₂ was not achieved. Results are presented in **Table 2**.

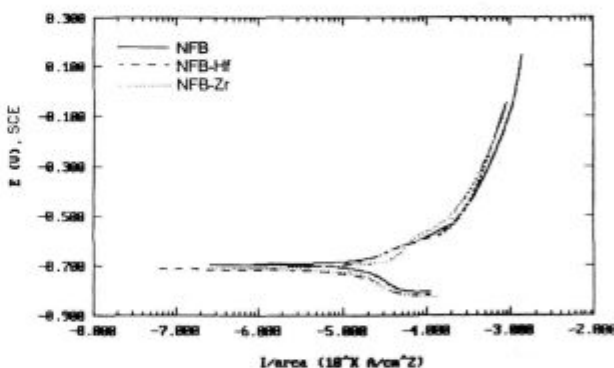


Figure 1: Potentiodynamic polarisation curves for three types of alloys tested in fresh water, 20°C

Table 1: Corrosion rates of alloys in different media at 20°C

Material	Media	Corrosion rate (mm/year)
NFB	fresh water	0,300
NFB-HfO ₂	fresh water	0,530
NFB-ZrO ₂	fresh water	0,022
NFB	0,09 M NaCl	2,120
NFB-HfO ₂	0,09 M NaCl	2,710
NFB-ZrO ₂	0,09 M NaCl	2,650
NFB	0,17 M NaCl	2,650
NFB-HfO ₂	0,17 M NaCl	3,260
NFB-ZrO ₂	0,17 M NaCl	3,150
NFB	0,5 M H ₂ SO ₄	303,0
NFB-HfO ₂	0,5 M H ₂ SO ₄	274,0
NFB-ZrO ₂	0,5 M H ₂ SO ₄	237,8

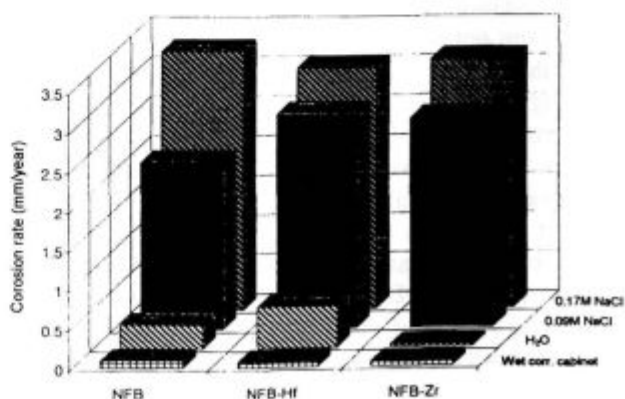


Figure 2: Corrosion rates of the materials exposed in various media presented graphically

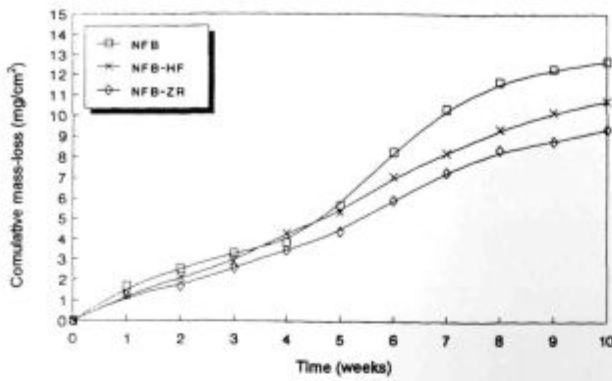


Figure 3: Cumulative mass-loss of different alloys during 10 weeks of exposure in a wet corrosion chamber

Table 2: Corrosion rates of alloys exposed in a wet corrosion cabinet

Material	Environment	Corrosion rate (mm/year)
NFB	Wet corrosion chamber	0,089
NFB-HfO ₂	Wet corrosion chamber	0,072
NFB-ZrO ₂	Wet corrosion chamber	0,063

3.2 Microstructural study

Cross section of the samples A, B, C were ground and polished with diamond paste. The polished surfaces were examined by optical microscopy and electron microscopy (SEI and BSEI). The phases present were analysed using EDS standardless quantitative analyses.

Figure 4 shows a comparison of the microstructures (cross sections) of sample without any addition (A) and sample with 1 wt.% of HfO₂ addition (B). Figure 5 shows the cross sections of the polished surfaces of samples with HfO₂ (B) and ZrO₂ (C) addition. There is an obvious difference in the level of corrosion attack between the three samples. The most aggressive corrosion

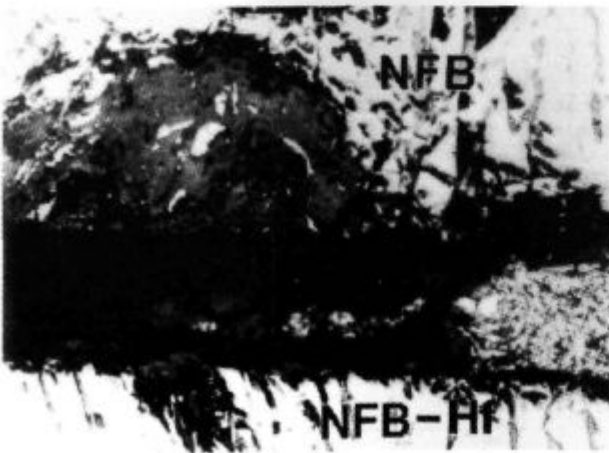


Figure 4: Microstructures (cross sections) of sample without any addition (A) and sample with 1 wt.% of HfO₂ (B) (385 x)

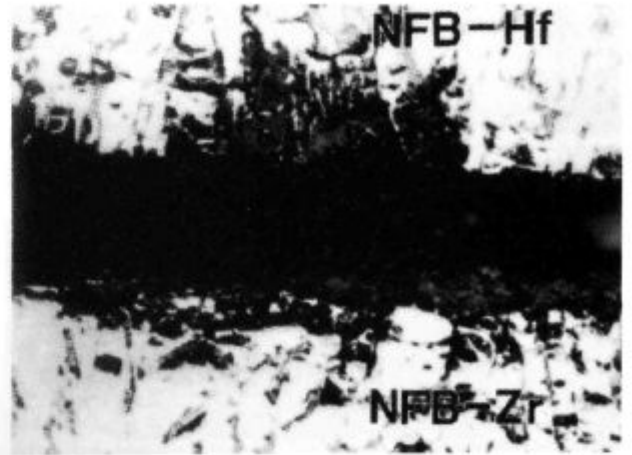


Figure 5: Microstructures (cross sections) of sample with HfO₂ (B) and sample with ZrO₂ (C) (385 x)

proceeds in samples A. In samples B and C the corrosion products are located mainly on the surface, especially in samples C, where no deep corrosion in the bulk material was observed. The reason for such local corrosion is supposed to be the presence of particular phases.

More detailed analyses of the phases present were obtained by electron microscopy. Figure 6 shows the combined BS/SE image of an SEM micrograph of sample A and spectra of phases P₁ and P₂. The phases present in the corrosion products of sample A were found to be combined Nd, Dy and Fe oxides. The ratio between Nd and Fe oxides differs in the phases P₁ and P₂. The results of standardless quantitative analyses (ZAF correction program) are presented in Table 3.

Table 3: The results of standardless quantitative analyses of the oxide phases

	Nd ₂ O ₃ (wt.%)	Dy ₂ O ₃ (wt.%)	FeO (wt.%)
Phase P ₁	43,35	30,18	24,47
Phase P ₂	07,69	-	92,31
Phase P ₁₁	37,55	24,73	37,72
Phase P ₁₂	11,99	-	88,01

In samples B a Hf-Fe rich phase was detected. The combined BS/SE image of the SEM micrograph of sample B and the corresponding spectrum of phase P₆ are shown in Figure 7. Other phases present are the matrix phase P₅ (RE₂Fe₁₄B) and RE -rich phase P₇.

In samples C a Zr-Fe -rich phase was found, mostly on the phase boundaries between the hard magnetic RE₂Fe₁₄B phase (P₅) and the RE -rich phase (P₇). A combined BS/SE image of the SEM micrograph of sample C and the corresponding spectrum of Zr-Fe -rich phase P₉ are shown in Figure 8. The SEM micrograph of the same sample showing different phases in the corroded area and the corresponding spectra of these phases are presented in Figure 9. In samples C, the barrier based on the Zr-Fe -rich phase, which exists between the

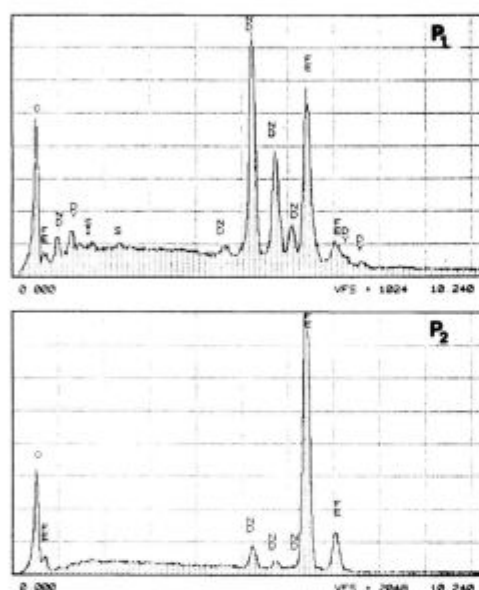
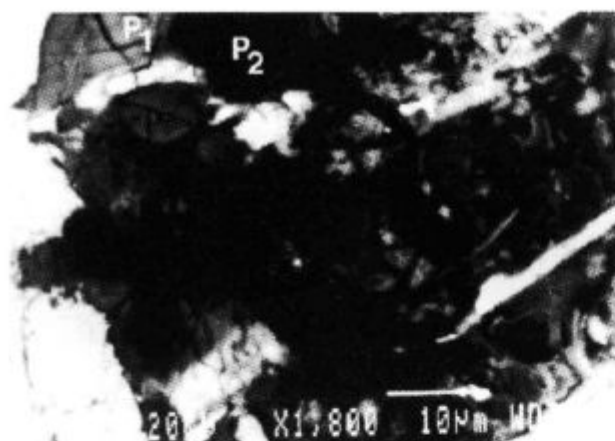


Figure 6: Combined BS/SE image of SEM micrograph of sample A and spectra of phases P₁ and P₂

corrosion products (in the RE -rich phase) and the hard magnetic matrix phase, prevents the propagation of corrosion. Phase P₁₀ shown on SEM micrograph (Figure 9) illustrates this tentative explanation. The results of standardless analyses of the Zr-Fe -rich phases found are presented in Table 4.

Table 4: The results of standardless quantitative analyses of Zr-Fe -rich phases

	Zr	Fe	Nd
Phase P ₉	44,22	54,02	05,76
Phase P ₁₀	37,28	54,35	08,38

4 Conclusion

The results of the corrosion experiments and analyses of RE-Fe-B-X alloys, as well as analyses of the corrosion products and microstructural observation and analyses show, that zirconia addition gives the most promising re-

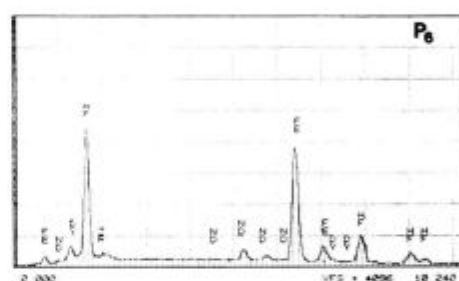
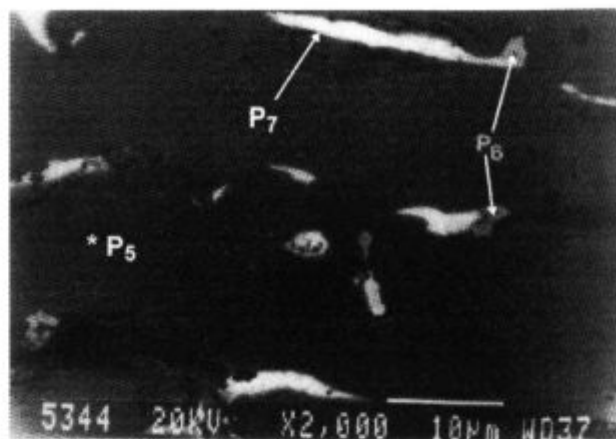


Figure 7: Combined BS/SE image of SEM micrograph of sample B and corresponding spectra of Hf-Fe -rich phase P₆

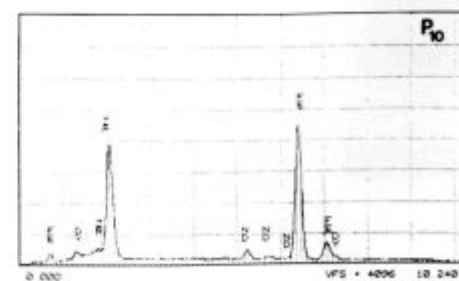
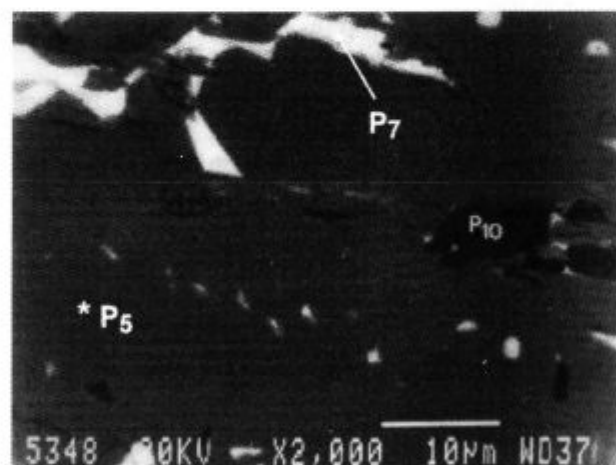


Figure 8: Back scattered image of SEM micrograph of sample C and the corresponding spectrum of Zr-Fe -rich phase P₁₀

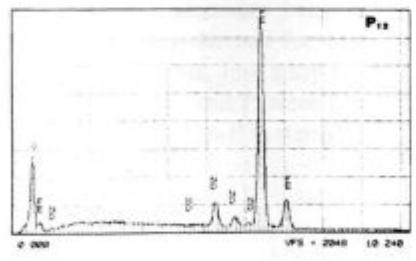
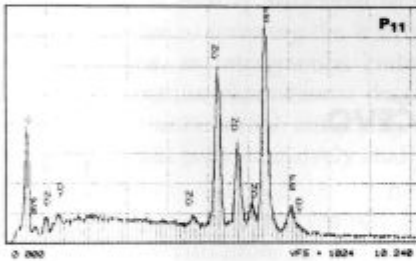
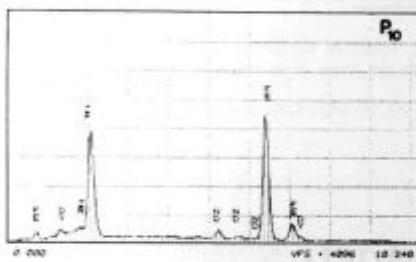
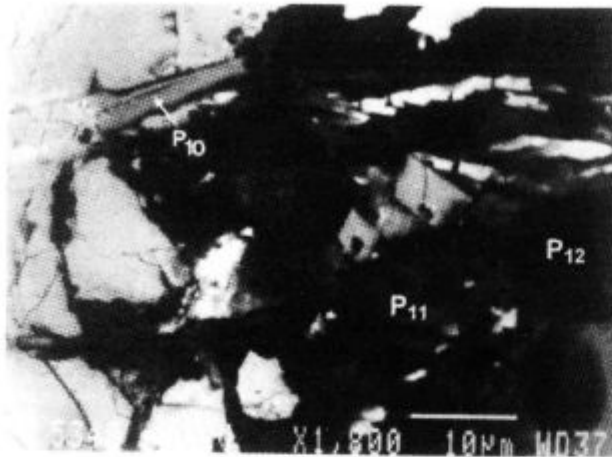


Figure 9: SEM micrograph of sample C showing various phases in the corroded area and the corresponding spectra of phases P₁₀, P₁₁ and P₁₂

sults in corrosion protection of the basic material. Corrosion rates in fresh water were 0,30 mm/year for Nd-Dy-Fe-B alloy and 0,02 mm/year for Nd-Dy-Fe-B-Zr alloy. The same trend was shown when the samples were exposed to conditions where condensed atmospheric humidity was simulated. The highest cumulative weight loss occurred with pure Nd-Dy-Fe-B alloys and the lowest with the alloy improved by ZrO₂ addition.

A tentative explanation for the difference is that the change in microstructure is obviously responsible for improving the corrosion resistance of Nd-Dy-Fe-B-Zr alloy. The reason for local corrosion is the presence of particular phases, (Fe-Hf, Fe-Zr) acting as an anode, with considerable potential difference between these and the matrix. A tentative explanation for the formation of Fe-Hf and Fe-Zr -rich phases is that in the samples with HfO₂ and ZrO₂ addition, during the arc melting process most probably Nd from Nd -rich phase reduces both oxides and Hf or Zr -rich phases are formed. They act as the barrier between the corrosion products (in the RE -rich phase) and the hard magnetic matrix phase and to some extent prevent the propagation of corrosion.

The improvement of the corrosion resistance of basic material itself can contribute significantly to the stability of coated magnetic material.

5 References

- ¹ M. Sagawa, S. Fujimura, N. Togawa, H. Yamamoto, Y. Matsuura, *J. of Appl. Phys.*, 55, 1984, 2083
- ² J. Croat, J. Herbst, J. Lee, F. Pinkerton, *J. of Appl. Phys.*, 55, 1984, 2078
- ³ M. Hersch, Permanent Magnet Demand Fuels Continued Market Growth, PCIM, July 1994, p 26
- ⁴ A. Kim, J. Jacobson, *IEEE Trans. on Mag.*, 23, 1987, 5,2509
- ⁵ A. Kim, *Journ. of Material Eng.*, 11, 1989, 1, 95
- ⁶ A. S. Kim, F. E. Camp, S. Constantinides, Corrosion of Electronic and Magnetic Materials, ASTM STP 1148, Ed. P. J. Peterson, Am. Soc. for Testing and Materials, Philadelphia, 1992, p 68
- ⁷ K. Narasimhan, C. Willman, E. Dulis, *US Patent*, No. 4588439, 1986
- ⁸ P. Tenaud, F. Vial, M. Sagawa, *IEEE Trans. on Magn.*, 26, 1990, 5, 1730
- ⁹ S. Hiroswawa, S. Tomizawa, S. Mino and A. Hamamura, *IEEE Trans. on Mag.*, 26, 1990, 5, 1960
- ¹⁰ S. Kobe Beseničar, J. Holc, G. Dražič, B. Saje, *IEEE Trans. on Mag.*, 30, 1994, 2, 693
- ¹¹ H. Nakamura, A. Fukuro, T. Yoneyama, *Proc. of the 10th Inter. Workshop on Rare Earth Magnets and Their Application*, Kyoto, Japan, 1989, p 315
- ¹² M. Sagawa, S. Fujimura, H. Yamamoto, S. Hiroswawa, *Japanese Patent*, No. 6338555, 1988